JOIV : Int. J. Inform. Visualization, 8(1) - March 2024 352-360

INTERNATIONAL JOURNAL ON INFORMATICS VISUALIZATION

journal homepage : www.joiv.org/index.php/joiv

Concept and Design of Anthropomorphic Robot Hand with a Finger Movement Mechanism based on a Lever for Humanoid Robot T-FLoW 3.0

Kevin Ilham Apriandy [a,c], Faiz Ulurrasyadi [b,c], Raden Sanggar Dewanto [b,c], Bima Sena Bayu Dewantara [a,c], Dadet Pramadihanto [a,c,*]

[a] *Dept. of Informatics and Computer Engineering, Politeknik Elektronika Negeri Surabaya (PENS), Sukolilo, Surabaya, 60111, Indonesia*
[b] *Dept. of Energy Mechanics Engineering, Politeknik Elektronika Negeri Surabaya (PENS), Sukolilo, Surabaya, 60111, Indonesia*
[c] *Robotics and Intelligent System Center (RoISC), Politeknik Elektronika Negeri Surabaya (PENS), Sukolilo, Surabaya, 60111, Indonesia*
Corresponding author: [*]dadet@pens.ac.id

***Abstract*— This work described a concept and design of an anthropomorphic robot hand for the T-FLoW 3.0 humanoid robot, which featured a mechanism based on a lever as its finger movement. This work aimed to provide an affordable, modular, lightweight, human-like robot hand with a mechanism that minimizes mechanical slippage. The proposed mechanism works based on the push/pull of a lever attached to the finger to generate its finger flexion/extension movement. The finger's lever is pushed/pulled through a servo horn and a rigid bar by the affordable TowerPro MG90S micro-servo. Our hand is developed only as necessary to become close to human hands by only applying five fingers and six joints, where each joint has its actuator. The combination of 3D printing technology with PLA filament accelerates and streamlines the manufacturing process, provides a realistic appearance, and achieves a lightweight, affordable, and easy maintenance product. Structural analysis simulations show that our finger design constructed with PLA material could withstand a load of about 30 N. We verified our finger mechanism by repeatedly flexing and extending the finger 30 times, and the results showed that the finger movements could be performed well. Our hand offered excellent handling for the mechanical issues brought on by finger movements, one of the issues that robot hand researchers have encountered. Our work could provide significant benefits to the T-FLoW 3.0 developers in enhancing the ability of humanoid robots involving hands, such as grasping and manipulating objects.**

***Keywords*— Humanoid robot FloW; anthropomorphic robot hand; finger movement mechanism based on a lever; kinematics analysis; static structural analysis.**

Manuscript received 5 May. 2023; revised 13 Jun. 2023; accepted 2 Oct. 2023. Date of publication 31 Mar. 2024.

I. Introduction

RoISC revolutionized the way of developing their FLoW humanoid robots, which were formerly only intended for entertainment but now also to provide assistance to people. Prominent changes were made from FLoW-1 [1] and FLoW-2 to T-FLoW 3.0 [2], [3] as a result of the revolution, with all revisions to its vision, middleware, controllers, degree-of-freedom configuration, and mechanical design. In addition to that, as shown in Fig. 1, in contrast to the previous two FLoW versions, the design concept of T-FLoW 3.0 is based on how to develop humanoid robots only as necessary to become close to humans. For all those reasons, one thing that RoISC did was to create an anthropomorphic robot hand for T-FLoW 3.0. It is expected that prominent changes like the addition of hands would enable T-FLoW 3.0 to accomplish RoISC's revolution goals, which are to develop humanoid robots only as necessary to become close to humans and assist people.

Outside of RoISC, the development of anthropomorphic robot hands has increased and become one of the most intriguing areas of study. As stated in [4], many researchers from various fields participate in developing robot hands, and each creates the hands according to their field. Ranging from the categories of human–robot interaction for service [5], social [6], entertainment [7], teleinteraction [8], and teleoperation [9], categories of rehabilitation for prosthetics [10] and assistive robotics [11], to the categories of industrial for autonomous manipulation [12], logistics [13] and supervised manipulation [14]. With so many variations, it is possible to create an optimal hand that solves particular issues

and approximates humans based on the benefits and drawbacks of each developed type.

In terms of how the fingers move, there are many ways to implement the idea, some of which utilize gears, linkages, and wires as their base mechanism. Researchers have come up with different approaches in these categories. Yoneda et al. [15] have implemented gear transmission mechanisms for its finger movements. Katsumaru et al. [16] have designed the transmission based on a gear series to lower the actuator's number. Lee et al. [17] brought their own self-modified "actuator modules" with numerous spur gears. Using a small mini-motor GA12-N20, notable research in [18] proposes a combination of bevel gear and tendon-driven to actuate the finger. Wahit et al. [19] suggested a finger mechanism using a solid connection to move the joint between the actuator and the robot frame. Kim et al. [20] have developed an integrated linkage-driven system consisting of a series of parallel mechanisms to implement movements at the finger joint. Nurpeissova et al. [21] presented a linkage-based driven with worm-and-rack transmission to actuate its finger. Next, Jeong et al. [22] relied on the dual-mode twisted string actuation mechanism and rotary-to-linear transmission to maintain lightweight and compactness. Ryu et al. [23] have developed an underactuated finger mechanism using a tendon-driven method to move its finger phalanges. Kontoudis et al. [24], [25] presented a versatile, adaptive finger that could execute flexion/extension and adduction/abduction using a tendon-based actuation mechanism.

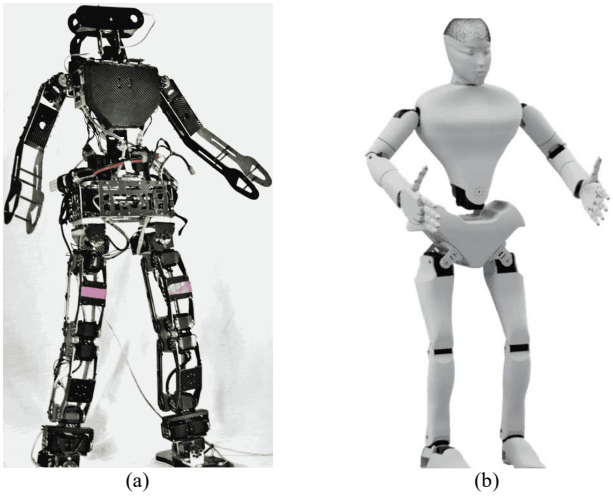

(a) (b)

Fig. 1 Humanoid robot FLoW through the generations (a) FLoW1 (2015) (b) T-FLoW 3.0 (2019)

With this work, we attempt to provide a new approach to RoISC for their development of the humanoid robot T-FLoW 3.0's hand, and we also want to contribute to the world regarding research on anthropomorphic robot hand by presenting an affordable, modular, and lightweight robot hand that has a finger movement mechanism based on a lever. The mechanism has previously been proposed in [26]; it works by pushing/pulling a lever attached to the finger using the affordable TowerPro MG90S micro servo. Our hand has six micro-servos in total, which correspond to all the joints in the hand, one for each joint of the finger and two for the joint of the thumb. Our hand would be manufactured with the technology of 3D printing to accelerate and streamline the manufacturing process and provide a realistic appearance. The use of PLA filament material in the manufacturing method is to achieve lightweight, affordable, and easy maintenance. Our proposed work proved to be effective in overcoming the issue of mechanical slip caused by finger movements, which, at the time, hampered the first approach [27] of the humanoid robot T-FLoW 3.0's hand.

II. Materials and Method

A. Hand Design Concept

Building an anthropomorphic robot hand is a highly complicated task since the design must endure so many levels of difficulty [28], [29]. The design must comply with the predefined size to have a good body proportion with the other parts of the robot [30], making it barely be designed flexibly. An inflexible size will only complicate the design even more, considering it contains many moving parts, joints, and supporting devices. Additionally, there currently need to be bigger actuators on the market, which would limit the space availability for the design and raise the mechanism complexity. Not to mention, the hand has to be designed with curves and shapes that are aesthetically beautiful to replicate the impeccability of the human hand, which takes an immense effort to accomplish. Competitive cost is the last crucial thing, as the robot hand could be used to replace the human hand in various situations.

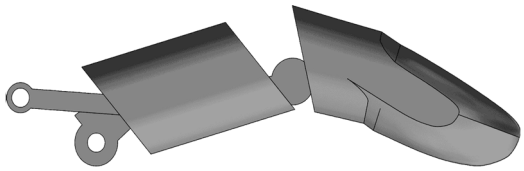

Fig. 2 The appearance of the humanoid robot T-FLoW 3.0's finger

Because of the inevitable trade-offs between size requirements and size restrictions of our anthropomorphic robot hand, simultaneously meeting all design demands, both functionality and proportionality, is highly challenging. Therefore, we strived to find a suitable compromise and optimal balance between the two, working towards seeking a configuration that would enable both sides to maximize the advantages. We are focusing the task on two primary aspects: outlining several requirements regarding function and structure and eliminating unimportant components to retain the size within the sensible limits. Correspondingly, it is assumed that only a few joints are essential, which leads the design to have only six degrees of freedom, one for each finger's base and two for the thumb. Although the elimination of several components makes our robot hand far from resembling the impeccability of a human hand in both appearance and function, we still endeavor to preserve the primary purpose of the hand intact, and it is still capable of performing main tasks such as pinching and grasping [31].

Our robot hand development guidelines are decided only as necessary to become close to humans by proposing a configuration of five fingers and six joints powered by six actuators. All fingers use the same design, from the thumb to the baby's finger. As shown in Fig. 2 above, the finger consists of one non-actuated type of inactive joint in the middle and one active joint at the base. Unlike the others, the thumb is

designed to have one non-actuated inactive kind of joint, two active joints, and one additional link (thenar part) to allow more agile hand movements. Since only one joint could be controlled, we bent the finger posture so the hand could perform pinching and grasping poses. The entire design of our anthropomorphic robot comprises the fingers, palm, and several supporting devices, as depicted in Fig. 3. For each finger joint, one micro-servo is lodged into the palm, and two for the thumb joint placed at the base of each thumb's link. Each micro-servo comes with a rigid bar and a servo horn to pull or push the finger-attached lever, aiming to move the fingers into the targeted position. Microcontroller Arduino Nano implements the systems and serves as the hand's brain for the movement. Our robot hand is built around the concept of an exoskeleton to provide more space for the placement of the components inside, as well as higher-level durability and strength to protect and cover the components within. To deliver results that are lightweight, affordable, and easy to maintain, all our hand materials would be manufactured using PLA filament. The latest computer-aided design and 3D printing technologies are used to design and manufacture our hands to get aesthetically fascinating contours, realistic appearances, and shapes that are barely possible to achieve with older technology.

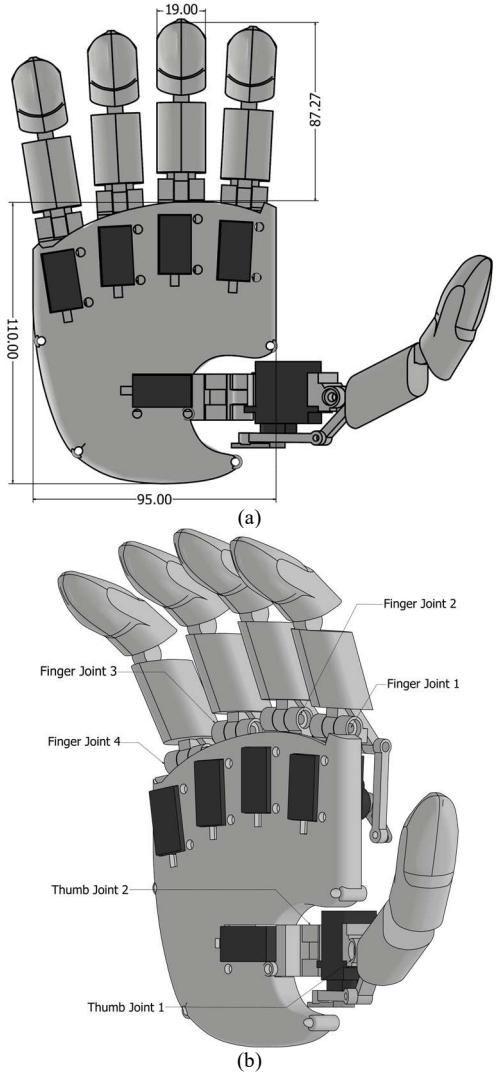

Fig. 3 Full appearance of the humanoid robot T-FLoW 3.0's hand (a) back view (b) isometric view

B. Finger Movement Mechanism based on a Lever

Looking back when building the old approach prototype of the humanoid robot T-FLoW 3.0's hand [27], the use of a Nylon Fishing Line (NFL) paired with a 3D printed PLA pulley occasionally made the mechanism slip when performing cable winding/unwinding and causes the unpredictable fingers movement. The mechanism is also a little bit tricky to assemble because the direction of the pulley is perpendicular to the direction of the finger flexion/extension rather than in the same direction as it is. Hence, the approach was immediately abandoned when its weaknesses emerged. Unfortunately, the old approach prototype of the humanoid robot T-FLoW 3.0's hand was no longer being developed; as such, the data regarding the weaknesses cannot be gathered empirically.

Reflecting on those experiences, we sought to strengthen those areas or, at the very least, achieve better outcomes. Aiming to eliminate mechanical slippage and create solid finger movements, we found a solution by proposing a finger movement mechanism based on a lever. A finger mechanism that works by attaching a lever to the base of the finger and then pulling/pushing it with a rigid bar to produce finger movement. Using a rigid bar makes the movement constant, and the potential performance loss owing to mechanical slippage would be much less. The fingers and mechanism are designed independently in a modular manner, as shown in Fig. 4, making it easy to assemble because the mechanism is not implanted in the palm.

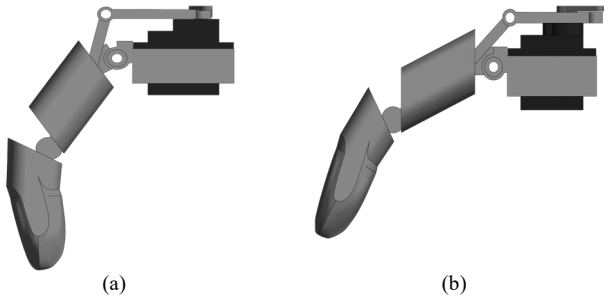

Fig. 4 The proposed finger movement mechanism for humanoid robot T-FLoW 3.0's hand (a) finger flexion (actuator push) (b) finger extension (actuator pull)

C. Actuator of the Finger

One of the most complex parts when creating the initial concept of our anthropomorphic robot hand with six actuators is determining the suitable actuators to use. When conceiving a finger movement mechanism, careful consideration should be given to the appropriate actuator that could maximize the potential of the finger mechanism. Similarly, when choosing an actuator, it must be well thought about what kind of suitable finger mechanism could maximize the actuator's potential. Using those considerations, the role of the actuators becomes crucial as it is closely related to the concept of our proposed robot hand and finger mechanism.

Instead of the popular angular type of mechanism, our actuation mechanism is the linear type. Thus, we are seeking an actuator that could generate linear motion for the requirement of pulling/pushing the finger's lever. Additionally, we are seeking a small and affordable actuator that provides good torque and operating speed. Two options fit all the abovementioned requirements, i.e., Actuonix PQ-

12P linear motor and TowerPro MG90S micro-servo. However, using the PQ-12P as an actuator would arguably violate the spirit of the competitive cost that we aspire to, as it has a high price and operates at a high voltage of 12V. Eventually, the MG90S micro-servo is ultimately chosen since it offers good operating speed and an affordable price. Another benefit of the MG90S micro-servo is its ability to run at 5V, making it convenient. The specifications of the MG90S micro-servo are shown in Table I below.

TABLE I
SPECIFICATION OF MG90S MICRO-SERVO ACTUATOR

Weight	:	13.4g
Stall Torque	:	1.8 kg. cm
Max Stall Torque	:	2.2 kg. cm (at 6.6V)
Operating Voltage	:	4.8V
Operating Speed	:	0.10 sec/60 degree (4.8V);
Rotation	:	0-180 degree
Dimension	:	22.8x12.2x28.5mm

D. Materials and Manufacturing

CAD (computer-aided design) has improved substantially in recent years, enabling researchers to create 3D models rapidly and efficiently. With such improvements, researchers need more boundaries in conveying their brilliant creative concepts when using computers. We are also excited to use those improvements to build an affordable, modular anthropomorphic robot hand with the look of realistically and aesthetically fascinating contours. However, turning digital models produced by computer-aided design (CAD) into actual parts could be challenging, mainly when using traditional manufacturing methods.

Therefore, we planned to use the latest technology in the implementation field by utilizing 3D printing as a manufacturing method. With the help of 3D printing, we could realize an idea, innovation, concept, invention, or anything digitally drawn in a relatively short time [32], turning it from an essential thought to an actual part. Geometry that was traditionally challenging to manufacture, such as unrealistic overhangs, is now considerably trouble-free and effortless. The widely used Polylactic Acid material further aids these conveniences. In the report of [33], merging the intrinsic properties of PLA with the technology of 3D printing was cited as a potential way to create bio-inspired complex products. In our proposed anthropomorphic robot hand, PLA is planned to be used as the primary material since it is affordable, easy to operate, easy to maintain, and lightweight. Table II below shows the specification of PLA provided by [33].

TABLE II
SPECIFICATION OF GENERIC POLYLACTIDE (PLA)

Thermal Conductivity	:	16.766E-02 W/(m °C)
Specific Heat	:	1.868333333 J/(g·°C)
Behavior	:	Isotropic
Young Modulus	:	1.28 GPa
Poisson Ratio	:	0.36
Shear Modulus	:	1287 MPa
Density	:	1.252 g/cm³
Yield Strength	:	70 MPa
Ultimate Tensile Strength	:	73 MPa

III. RESULTS AND DISCUSSION

A. Static Structural Analysis Simulation of Finger Design

After creating the design of our anthropomorphic robot by hand using CAD (computer-aided design), the next stage was to use CAE (computer-aided engineering) to evaluate its strength. The design's strength was assessed to identify where the potential failure points would occur by simulating the structural loading conditions using Autodesk Inventor's static stress analysis. The fingertip was simulated because we consider it to be the part that suffers the most load distribution when the hand performs pinching and grasping movements. The simulations aim to evaluate the ability of the finger design to sustain the load coming from the upward direction. Three different simulation result types—Safety Factor, Displacement, and Von Mises Stress— were analyzed in this section, and the applied load to this simulation is set up from 3 N and gradually increases to 30 N. The simulation results for static stress analysis are displayed in Table III.

TABLE III
RESULT OF THE SIMULATION OF STATIC-STRESS ANALYSIS

No.	Load (N)	Type	Von Misses Stress (MPa)	Displacement (mm)
1.	3	Minimum	0	0
		Maximum	6.132	0.723
2.	6	Minimum	0	0
		Maximum	12.264	1.45
3.	9	Minimum	0	0
		Maximum	18.396	2.17
4.	12	Minimum	0	0
		Maximum	24.528	2.89
5.	15	Minimum	0	0
		Maximum	30.66	3.61
6.	18	Minimum	0	0
		Maximum	36.792	4.34
7.	21	Minimum	0	0
		Maximum	42.924	5.06
8.	24	Minimum	0	0
		Maximum	49.056	5.78
9.	27	Minimum	0	0
		Maximum	55.188	6.51
10.	30	Minimum	0	0
		Maximum	61.32	7.23

Based on the simulation results using Autodesk Inventor's static stress analysis and the PLA material parameters provided by [33], it is found that as the load increases, the red-highlighted joint region in Fig. 5 (a) and (c) is projected as the possible failure point. With the safety factor's tolerance set at 1.1, it is presumed that the finger design could withstand a load of up to 30 N. A low safety factor is deemed acceptable if the design fails without endangering living things. If the applied load continues to increase gradually until it reaches the destructive testing condition (73 MPa), then the proposed finger design is predicted to fail at a load of 35.7 N. The results of the simulation are visualized in the following Fig. 5 (a), (b) and (c).

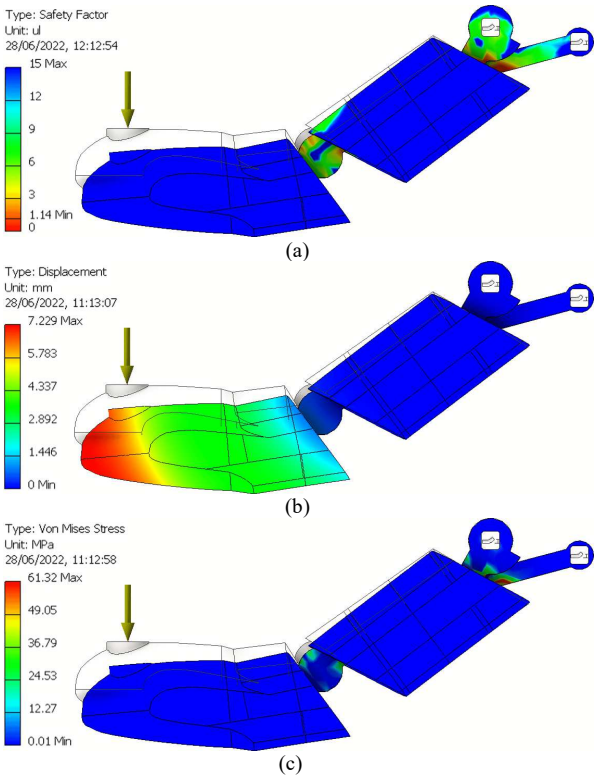

Fig. 5 Static-stress analysis simulation results of the finger design with an applied load of 30 N (a) Safety Factor (b) Displacement (c) Von Mises Stress

B. The Range and Maximum Angle of each Joint of the Hand Design

The range and maximum angle of each finger joint should be determined to ensure that the mechanism doesn't reach an excessive angle, which might cause mechanical damage to the actuator and the robot. The joint angles of the index, middle, ring, and baby finger were defined at a range of 66°, according to the average angle of the joint boundaries from the simulation in our previous work [26]. Especially for the two joints of the thumb, the range of the angles is set at 66° and 85° to provide more agile hand movements. A barrier was delivered in the joint region so that when the mechanism exceeds a maximum angle, the joint region will hold, protecting the finger from mechanical harm. The barrier is shown in Fig. 6 (a) and (b) below.

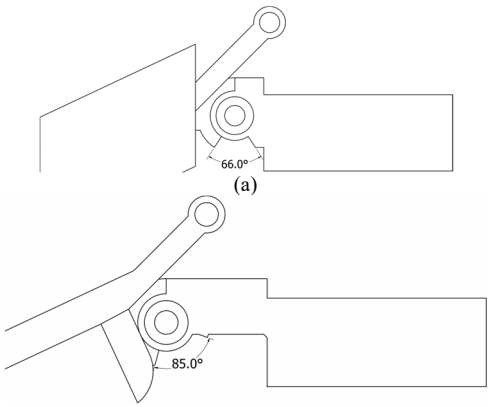

Fig. 6 The angle range of the finger joint of humanoid robot T-FLoW 3.0 (a) the joint 1 of the thumb, and the joint of the index, middle, ring, and baby finger (b) the joint 2 of the thumb

Autodesk Inventor's dynamic simulation was used to evaluate the collisions that might occur between the fingers and palm when the robot hand performs its fundamental tasks: pinching and grasping, as depicted in Fig. 7. The simulation results indicate that the joint region would hold just before the collision, protecting the fingers and palm from mechanical harm. However, the collision between the thumb and finger cannot be prevented with a barrier since doing so would restrict the thumb's range of movement. Thus, we will avoid the collision by using several lines of code written on the hand operating system.

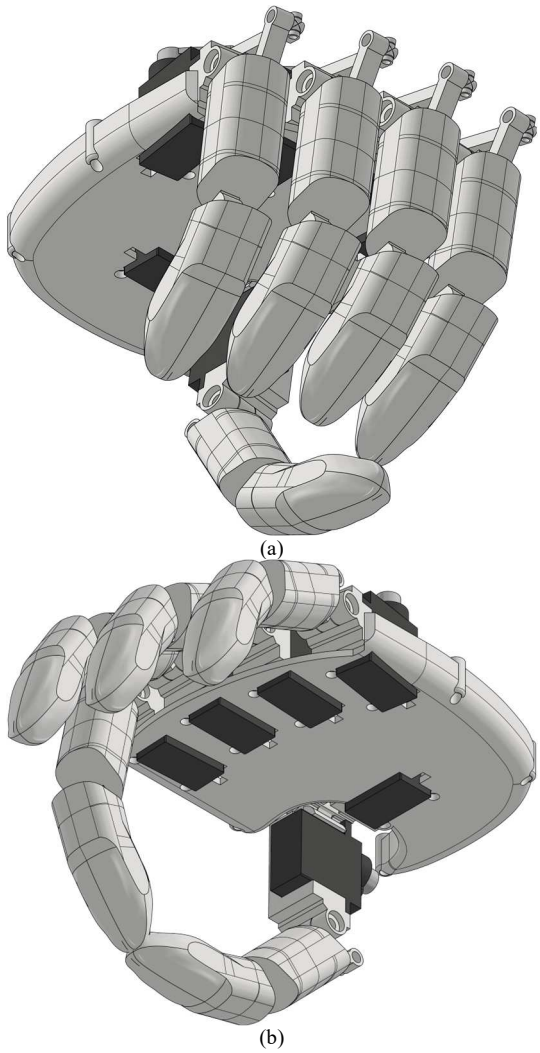

Fig. 7 The looks of humanoid robot T-FLoW 3.0's hand (a) during the grasping condition and (b) during the pinching condition

C. Kinematics and Range of Motion of the Finger Design

The pose (position and orientation) of the end-of-effector of the finger is constantly changed due to the movement of the joint. Hence, kinematic analysis is required to predict the pose of the end-of-effector of the finger based on the changes in the joint value. The analysis was performed using forward kinematics to derive the kinematics model of the finger. In this analysis, the variable value is only the joint value ($\theta_{Finger}/\theta_{Thumb}$), and the constant value is the length of the link of the finger.

Based on the finger's kinematics design shown in Fig. 8 (a) below, the end-of-effector position of the finger can be

obtained by rotating (25+θ_{Finger}) degrees on the x-axis, and translating -40.5 mm on the z-axis, then rotating 32.63 degrees on the x-axis, and translating -45.249 mm on the z-axis, respectively, from the finger base R. Then, from the kinematics design, forward kinematics of the finger could be determined using the homogeneous transformation method, and the mathematical equation could be seen in equation (1). From equation (1), the position vector of the finger's end-of-effector could be calculated with equation (2).

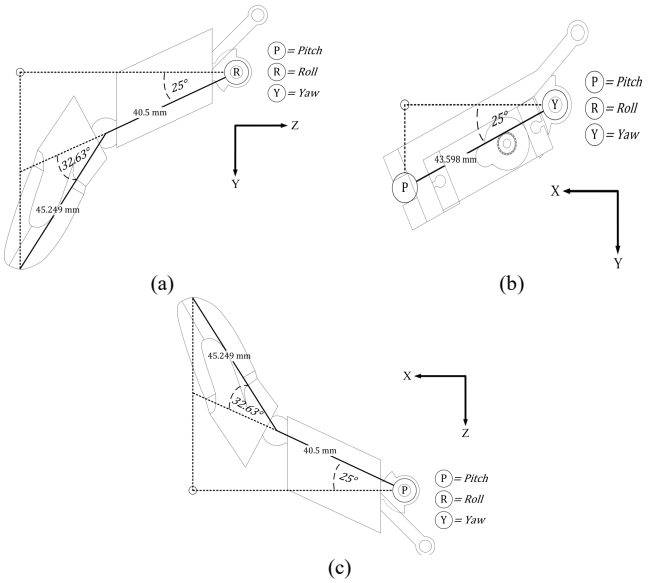

Fig. 8 The kinematics design of each part of the hand (a) Kinematics design of humanoid robot T-FloW 3.0's finger (b) Kinematics design of the first step of humanoid robot T-FloW 3.0's thumb (thenar part) (c) Kinematics design of the second step of humanoid robot T-FloW 3.0's thumb (thumb part)

Since the index, middle, ring, and baby fingers of the humanoid robot T-FloW 3.0's hand are identically shaped and located on the same plane, they could be illustrated using the same kinematics design. The purpose of illustrating kinematics design is to facilitate the construction of kinematics equations so that the modeling will be easier, and it could be known what parameters are required. The actual position of the finger in the real-world scene is located on the z-y plane, so the kinematics design of the finger is interpreted in the z-y plane. Using the joint boundaries obtained in the previous simulation the finger design's RoM (Range of Motion) is divided into six movements. Starting from the finger's initial position (θ_{Finger} = 0), the angle steadily increases by 11° until it reaches 66°. The result of the ROM of the finger design is simulated and shown in Fig. 9 (a), based on the kinematics analysis in equations (1) and (2) below.

$$EoE_{Finger} = R_x(25+\theta_{Finger}) \cdot T_z(-40.5) \cdot R_x(32.63) \cdot T_z(-45.249) \quad (1)$$

$$EoE_{Finger(x,y,z)} = EoE_{Finger} \times [0,0,0,1]^T \quad (2)$$

$$J1_{Thumb} = R_z(25+\theta_{Thumb,2}) \cdot T_x(43.598) \quad (3)$$

$$EoE_{Thumb} = J1_{Thumb} \cdot R_y(25+\theta_{Thumb,1}) \cdot T_x(40.5) \cdot R_y(32.63) \cdot T_x(45.249) \quad (4)$$

$$J1_{Thumb(x,y,z)} = J1_{Thumb} \times [0,0,0,1]^T \quad (5)$$

$$EoE_{Thumb(x,y,z)} = EoE_{Thumb} \times [0,0,0,1]^T \quad (6)$$

In thumb analysis, based on the thumb's kinematics design shown in Fig. 8 (b) and (c), the procedure consists of two steps to get to the position of the thumb's end-of-effector, i.e. thenar and thumb part. The first step is from the thumb base Y to the thumb joint 1 P (thenar part), then the second step is from the thumb joint 1 P to the thumb's end-of-effector (thumb part). In the first step, the thumb joint 1 P position can be obtained by rotating (25+ $\theta_{Thumb,2}$) degrees on the z -axis and translating 43.598 mm on the x-axis, from the thumb base Y. In the second step, the end-of-effector position of the thumb can be obtained by rotating (25+$\theta_{Thumb,1}$) degrees on the y-axis, and translating 40.5 mm on the x-axis, then rotating 32.63 degrees on the y-axis, and translating 45.249 mm on the x-axis, respectively, from the thumb joint 1 P. From the kinematics design, the forward kinematics of the thumb could be determined using the homogeneous transformation method, and the mathematical equation could be seen in equations (3) and 4). From equation (3), (4), the position vector of the thumb joint 1 P and the thumb's end-of-effector could be calculated with equation (5), (6).

The actual position of the thumb ©n the real-world scene is located on the x-y and x-z plane, so the kinematics are interpreted in the x-y and x-z plane. By using the joint boundaries obtained in the simulation before, the RoM (Range of Motion) of the thumb design is divided into five movements for $\theta_{Thumb,2}$ (thenar part) and six movements for $\theta_{Thumb,1}$ (thumb part). For the first RoM (thenar part), starting from the thumb's initial position ($\theta_{Thumb,1}$ = 0 and $\theta_{Thumb,2}$ = 0), and then the $\theta_{Thumb,2}$ increases by 17° until it reaches 85°. The second RoM (thumb part), starting from the thumb's initial position ($\theta_{Thumb,1}$ = 0 and $\theta_{Thumb,2}$ = 0), and then the $\theta_{Thumb,1}$ increases by 11° until it reaches 66°. The result of the RoM of the thumb design is simulated and shown in Fig. 9 (b) and (c), based on the kinematics analysis in equations (3), (4), (5), and (6) above.

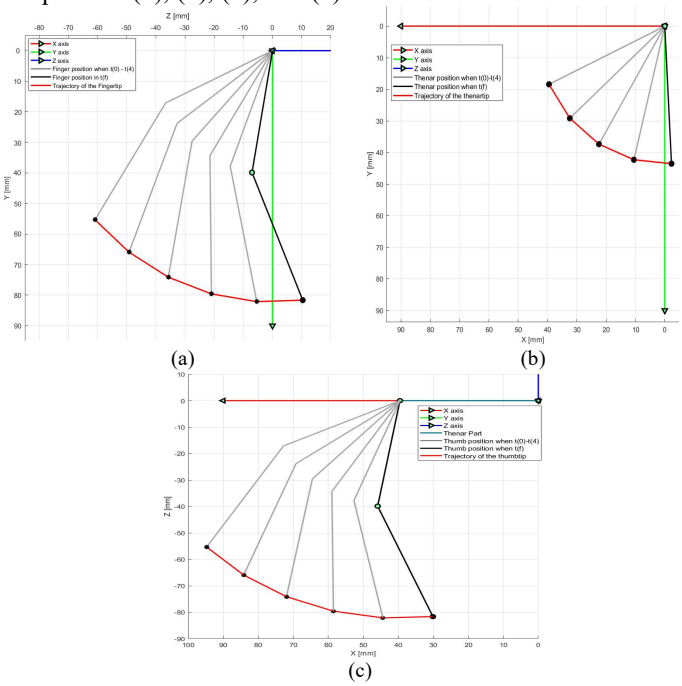

Fig. 9 The Region of Motion (RoM) of each part of the hand in each of its planes (a) The RoM of T-FLoW 3.0's finger in z-y plane (b) The first RoM (thenar part) of T-FLoW 3.0's thumb in x-y plane (c) The second RoM (thumb part) of T-FLoW 3.0's thumb in x-z plane

D. Linear Interpolation Model of the Proposed Finger Movement Mechanism based on a Lever

Instead of moving the finger joint directly, our mechanism moves the joint by pulling/pushing the finger's lever through a rigid bar and a servo-horn. Therefore, to place the finger joint into the targeted angle, it is necessary to model the mechanism, to find the correlation between the joint and servo-horn angle. In this case, linear interpolation will be used to model the correlation based on the minimum and maximum angles of the finger joint and servo-horn when the finger is in flexion and extension movement.

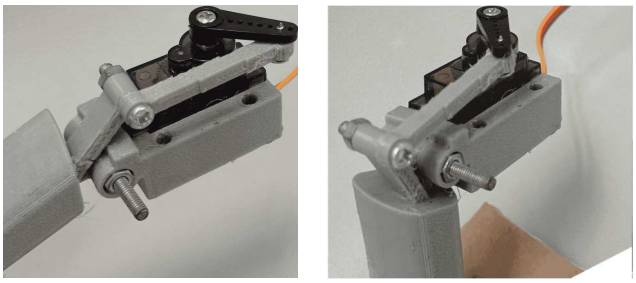

(a) (b)

Fig. 10 The position of the mechanism when the finger is in extension and flexion movement (a) The initial position of the mechanism when the finger is in extension movement (b) The final position of the mechanism when the finger is in flexion movement

Based on Fig. 6 (a), the minimum and maximum angles of the finger joint are already established. Then, the minimum and maximum angles of the finger servo-horn could be obtained by measuring the angles required by the servo when the mechanism performs finger extension (initial position) and finger flexion (final position), as shown in the Fig. 10 (a) and (b) above. The minimum and maximum angles of the finger joint and servo-horn could be seen in Table IV.

TABLE IV
THE COMPARISON OF THE RANGE ANGLE BETWEEN SERVO-HORN AND FINGER JOINT

Rotation	Range	
	Minimum	Maximum
Joint of the Finger	0	66
Actuator Horn	0	90

By using the linear interpolation model as in equation (7), the correlation between the finger joint and servo-horn angle could be solved using equations (8). According to equation (8), the finger joint is the input value x_{Finger}, and servo-horn is the output value y_{Finger}.

TABLE V
THE COMPARISON OF THE RANGE ANGLE BETWEEN ACTUATOR HORN AND JOINT 2 OF THE THUMBS

Rotation	Range	
	Minimum	Maximum
Joint 2 of the Thumb	0	85
Actuator Horn	0	100

In the thenar analysis, using the same method as before, linear interpolation will be used to model the correlation based on the minimum and maximum angles of the thumb joint 2 and servo-horn when the thenar is in flexion and extension movement. Based on Fig. 6 (b), The minimum and maximum angles of the thumb joint 2 are already established. Then, the minimum and maximum angles of the thenar servo-horn could be obtained by measuring the angles required by the servo when the mechanism performs thenar extension (initial position) and thenar flexion (final position), as shown in the Fig. 11 (a) and (b) below. The minimum and maximum angles of the thumb joint 2 and servo-horn could be seen in Table V.

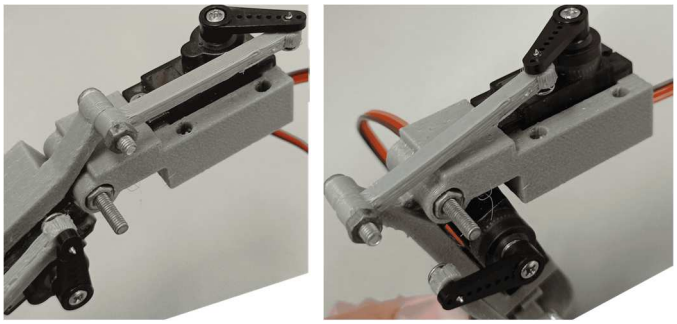

(a) (b)

Fig. 11 The position of the mechanism when the thenar is in extension and flexion movement (a) The initial position of the mechanism when the thenar is in extension movement (b) The final position of the mechanism when the thenar is in flexion movement

By using linear interpolation model as in equation (7), the correlation between the thumb joint 2 and servo-horn angle could be solved using equation (9). According to equation (9), thumb joint 2 is the input value x_{Thenar}, and servo-horn is the output value y_{Thenar}.

$$y = y_0 + (x - x_0)\,{(y_1 - y_0)}/{(x_1 - x_0)} \tag{7}$$

$$y_{Finger} = 0 + (x_{Finger} - 0)\,{(90 - 0)}/{(66 - 0)} \tag{8}$$

$$y_{Thenar} = 0 + (x_{Thenar} - 0)\,{(100 - 0)}/{(85 - 0)} \tag{9}$$

E. The Effectiveness of the Proposed Finger Movement Mechanism in Moving the Finger

The objective of this sub-section is to evaluate the effectiveness of our proposed finger movement mechanism based on a lever so that if there are any problems or anomalies in the movement of the finger, they can be known and observed. This experiment is also to prove whether it could answer the main problem brought up by this work, which is addressing the issue of mechanical slip caused by finger movements that, at the time, hampered the first approach of the humanoid robot T-FloW 3.0's hand. Experiments were carried out in the real world by realizing the prototype of the finger and its mechanism using 3D printing and PLA material.

The parameter used to determine the effectiveness of the mechanism is by observing whether the mechanism could perform flexion/extension movements to the finger properly, as exemplified in Fig. 4. As could be seen in Fig. 12 (a) and (b), the experiment was conducted by hanging the finger with a fixed point on the finger holder, and then the finger is performed to achieve flexion/extension finger movements. The procedure to evaluate the mechanism is by performing a combination movement of flexion/extension to the finger 30 times and observing whether any movement anomalies

occurred during the experiment. The results show that the proposed mechanism works well, and the finger can perform flexion/extension movements correctly. For more details, please have a look at https://youtube/SRCNMsqoUhk.

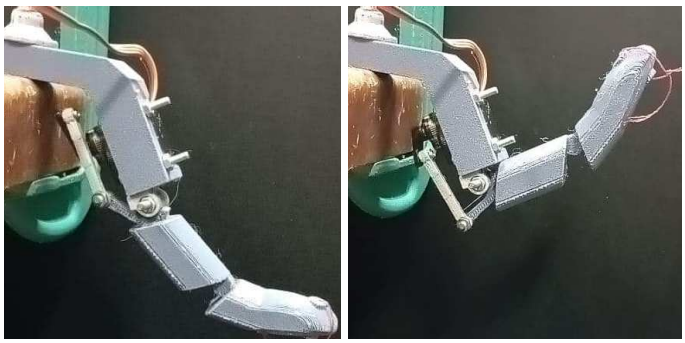

(a) (b)

Fig. 12 Result of the finger mechanism effectiveness experiment (a) The finger when successfully performing flexion (b) The finger when successfully performing extension

IV. Conclusions

We have successfully designed a new anthropomorphic robot hand as a new approach to the development of the humanoid robot T-FLoW 3.0's hand. Our proposed robot hand has a finger movement mechanism based on a lever, which works by pushing/pulling the finger lever to achieve flexion/extension finger movement. We were applied with five fingers, six joints, and six actuators since it was developed only as necessary to become close to human hands. 3D printing technology with PLA filament material was used to accelerate manufacturing, provide a realistic appearance, and produce a lightweight, affordable, and maintenance robot hand. To prevent the hand from mechanical harm caused by excessive control, we designed a mechanical stopper as a joint protector placed at the joint of each finger. Our proposed robot hand is intended to be easily assembled. Hence, our proposed finger movement mechanism based on a lever is designed modularly, independently, and separately from the palm. The finger we developed is designed to withstand a load of up to 35.7 N, according to static structural analysis simulations. Finally, we verified the effectiveness of our proposed finger movement mechanism in moving the finger by performing a combination of finger flexion/extension movements. Based on the experimental results, the finger movements could be carried out well using our finger movement mechanism based on a lever. Our approach successfully overcame the mechanical slip issues caused by finger movements that, at the time, hindered the first approach of the humanoid robot T-FLoW 3.0's hand.

With all these advantages, our approach is expected to contribute to two related fields of humanoid hand: robotics and prosthetics. Since our anthropomorphic robot hand is projected to have a wide range of applications, it might also be applied as a replacement for human hands in various situations. Consequently, developing our robot hand would be immensely beneficial for the good of humankind. However, with all of the above results, our robot hand is estimated to only accomplish some specific fundamental tasks and poses, and there is a lack of flexibility in movement that can be achieved, as our anthropomorphic robot only has a limited number of joints (DoF). Therefore, for our long-term work, the DoF would be increased so that our robotic hand would be capable of more diverse movements. For our short-term works, the concept of our proposed anthropomorphic robot hand would be manufactured and realized, and all the simulation tests would be empirically proved.

References

[1] V. C. P. H. Putra, K. I. Apriandy, D. Pramadihanto, and A. R. Barakbah, "FLoW-Vision: Object Recognition and Pose Estimation System based on Three-Dimensional (3D) Computer Vision," 2021 International Electronics Symposium (IES), Sep. 2021, doi:10.1109/ies53407.2021.9593994.

[2] W. Dewandhana, K. I. Apriandy, B. S. B. Dewantara, and D. Pramadihanto, "Forward Kinematics with Full-Arm Analysis on 'T-FLoW' 3.0 Humanoid Robot," 2021 International Electronics Symposium (IES), Sep. 2021, doi: 10.1109/ies53407.2021.9594017.

[3] F. Ulurrasyadi, R. S. Dewanto, A. Barakbah, and D. Pramadihanto, "Walking Gait Learning for 'T-FLoW' Humanoid Robot Using Rule-Based Learning," 2021 International Electronics Symposium (IES), Sep. 2021, doi: 10.1109/ies53407.2021.9593960.

[4] C. Piazza, G. Grioli, M. G. Catalano, and A. Bicchi, "A Century of Robotic Hands," Annual Review of Control, Robotics, and Autonomous Systems, vol. 2, no. 1, pp. 1–32, May 2019, doi:10.1146/annurev-control-060117-105003.

[5] D. Pavlichenko, D. Rodriguez, M. Schwarz, C. Lenz, A. S. Periyasamy, and S. Behnke, "Autonomous Dual-Arm Manipulation of Familiar Objects," 2018, doi: 10.48550/ARXIV.1811.08716.

[6] A. K. Pandey and R. Gelin, "A Mass-Produced Sociable Humanoid Robot: Pepper: The First Machine of Its Kind," IEEE Robotics & Automation Magazine, vol. 25, no. 3, pp. 40–48, Sep. 2018, doi:10.1109/mra.2018.2833157.

[7] J. A. E. Hughes, P. Maiolino, and F. Iida, "An anthropomorphic soft skeleton hand exploiting conditional models for piano playing," Science Robotics, vol. 3, no. 25, Dec. 2018, doi:10.1126/scirobotics.aau3098.

[8] S. Shigemi, "ASIMO and Humanoid Robot Research at Honda," Humanoid Robotics: A Reference, pp. 55–90, Oct. 2018, doi:10.1007/978-94-007-6046-2_9.

[9] H. Stuart, S. Wang, O. Khatib, and M. R. Cutkosky, "The Ocean One hands: An adaptive design for robust marine manipulation," The International Journal of Robotics Research, vol. 36, no. 2, pp. 150–166, Feb. 2017, doi: 10.1177/0278364917694723.

[10] M. Controzzi et al., "Progress Towards the Development of the DeTOP Hand Prosthesis: A Sensorized Transradial Prosthesis for Clinical Use," Converging Clinical and Engineering Research on Neurorehabilitation III, pp. 103–106, Oct. 2018, doi: 10.1007/978-3-030-01845-0_20.

[11] T. Wang, Z. Geng, B. Kang, and X. Luo, "Eagle Shoal: A new designed modular tactile sensing dexterous hand for domestic service robots," 2019 International Conference on Robotics and Automation (ICRA), May 2019, doi: 10.1109/icra.2019.8793842.

[12] M. Bartoš, V. Bulej, M. Bohušík, J. Stanček, V. Ivanov, and P. Macek, "An overview of robot applications in automotive industry," Transportation Research Procedia, vol. 55, pp. 837–844, 2021, doi:10.1016/j.trpro.2021.07.052.

[13] Y.-J. Kim, H. Song, and C.-Y. Maeng, "BLT Gripper: An Adaptive Gripper With Active Transition Capability Between Precise Pinch and Compliant Grasp," IEEE Robotics and Automation Letters, vol. 5, no. 4, pp. 5518–5525, Oct. 2020, doi: 10.1109/lra.2020.3008137.

[14] H. Park, M. Kim, B. Lee, and D. Kim, "Design and Experiment of an Anthropomorphic Robot Hand for Variable Grasping Stiffness," IEEE Access, vol. 9, pp. 99467–99479, 2021, doi:10.1109/access.2021.3094060.

[15] T. Yoneda, D. Morihiro, and R. Ozawa, "Development of a multifingered robotic hand with the thenar grasp function," Advanced Robotics, vol. 34, no. 10, pp. 661–673, Apr. 2020, doi:10.1080/01691864.2020.1751706.

[16] A. Katsumaru and R. Ozawa, "Design of 3D-printed assembly mechanisms based on special wooden joinery techniques and its application to a robotic hand," 2020 IEEE International Conference on Robotics and Automation (ICRA), May 2020, doi:10.1109/icra40945.2020.9197475.

[17] D.-H. Lee, J.-H. Park, S.-W. Park, M.-H. Baeg, and J.-H. Bae, "KITECH-Hand: A Highly Dexterous and Modularized Robotic Hand," IEEE/ASME Transactions on Mechatronics, vol. 22, no. 2, pp. 876–887, Apr. 2017, doi: 10.1109/tmech.2016.2634602.

[18] L. Liow, A. B. Clark, and N. Rojas, "OLYMPIC: A Modular, Tendon-Driven Prosthetic Hand With Novel Finger and Wrist Coupling Mechanisms," IEEE Robotics and Automation Letters, vol. 5, no. 2, pp. 299–306, Apr. 2020, doi: 10.1109/lra.2019.2956636.

[19] M. A. Abdul Wahit, S. A. Ahmad, M. H. Marhaban, C. Wada, and L. I. Izhar, "3D Printed Robot Hand Structure Using Four-Bar Linkage Mechanism for Prosthetic Application," Sensors, vol. 20, no. 15, p. 4174, Jul. 2020, doi: 10.3390/s20154174.

[20] U. Kim et al., "Integrated linkage-driven dexterous anthropomorphic robotic hand," Nature Communications, vol. 12, no. 1, Dec. 2021, doi: 10.1038/s41467-021-27261-0.

[21] A. Nurpeissova, T. Tursynbekov, and A. Shintemirov, "An Open-Source Mechanical Design of ALARIS Hand: A 6-DOF Anthropomorphic Robotic Hand," 2021 IEEE International Conference on Robotics and Automation (ICRA), May 2021, doi:10.1109/icra48506.2021.9561977.

[22] S. H. Jeong, K.-S. Kim, and S. Kim, "Designing Anthropomorphic Robot Hand With Active Dual-Mode Twisted String Actuation Mechanism and Tiny Tension Sensors," IEEE Robotics and Automation Letters, vol. 2, no. 3, pp. 1571–1578, Jul. 2017, doi:10.1109/lra.2017.2647800.

[23] W. Ryu, Y. Choi, Y. J. Choi, and S. Lee, "Development of a Lightweight Prosthetic Hand for Patients with Amputated Fingers," Applied Sciences, vol. 10, no. 10, p. 3536, May 2020, doi:10.3390/app10103536.

[24] G. P. Kontoudis, M. Liarokapis, and K. G. Vamvoudakis, "A Compliant, Underactuated Finger for Anthropomorphic Hands," 2019 IEEE 16th International Conference on Rehabilitation Robotics (ICORR), Jun. 2019, doi: 10.1109/icorr.2019.8779435.

[25] G. P. Kontoudis, M. Liarokapis, K. G. Vamvoudakis, and T. Furukawa, "An Adaptive Actuation Mechanism for Anthropomorphic Robot Hands," Frontiers in Robotics and AI, vol. 6, Jul. 2019, doi:10.3389/frobt.2019.00047.

[26] K. I. Apriandy, B. Sena Bayu Dewantara, R. S. Dewanto, and D. Pramadihanto, "Mechanical Design and Forward Kinematics Analysis of T-FLoW 3.0 Prosthetic Robot Hand: Lever-based Finger Movement Mechanism," 2022 International Electronics Symposium (IES), Aug. 2022, doi: 10.1109/ies55876.2022.9888385.

[27] Y. Bachtiar, R. D. Pristovani, S. Dewanto, and D. Pramadihanto, "Mechanical and Forward Kinematic Analysis of Prosthetic Robot Hand for T-FLoW 3.0," 2018 International Electronics Symposium on Engineering Technology and Applications (IES-ETA), Oct. 2018, doi:10.1109/elecsym.2018.8615522.

[28] P. Cerveri, N. Lopomo, A. Pedotti, and G. Ferrigno, "Derivation of Centers and Axes of Rotation for Wrist and Fingers in a Hand Kinematic Model: Methods and Reliability Results," Annals of Biomedical Engineering, vol. 33, no. 3, pp. 402–412, Jan. 2005, doi:10.1007/s10439-005-1743-9.

[29] G. Stillfried, "Movement model of a human hand based on magnetic resonance imaging (MRI)".

[30] S. Pheasant and C. M. Haslegrave, Bodyspace. CRC Press, 2018. doi:10.1201/9781315375212.

[31] F. Cini, V. Ortenzi, P. Corke, and M. Controzzi, "On the choice of grasp type and location when handing over an object," Science Robotics, vol. 4, no. 27, Feb. 2019, doi: 10.1126/scirobotics.aau9757.

[32] L. Somappa et al., "Design and Development of a Robotic Hand with Embedded Sensors Using 3D Printing Technology," Transactions of the Indian National Academy of Engineering, Jan. 2021, doi:10.1007/s41403-021-00198-y.

[33] S. Farah, D. G. Anderson, and R. Langer, "Physical and mechanical properties of PLA, and their functions in widespread applications — A comprehensive review," Advanced Drug Delivery Reviews, vol. 107, pp. 367–392, Dec. 2016, doi: 10.1016/j.addr.2016.06.012.